ACS OMEGA

Open Access

http://pubs.acs.org/journal/acsodf

Article

Effect of Strontium Modification in Mg−Al Mixed Oxide Catalysts on Product Distribution toward Catalytic Reaction of Ethanol

Patchaporn Seekhiaw, Sasiradee Jantasee, Piyasan Praserthdam, and Bunjerd Jongsomjit*

Cite This: *ACS Omega* 2023, 8, 32775−32783

Read Online

ACCESS | Metrics & More | Article Recommendations | Supporting Information

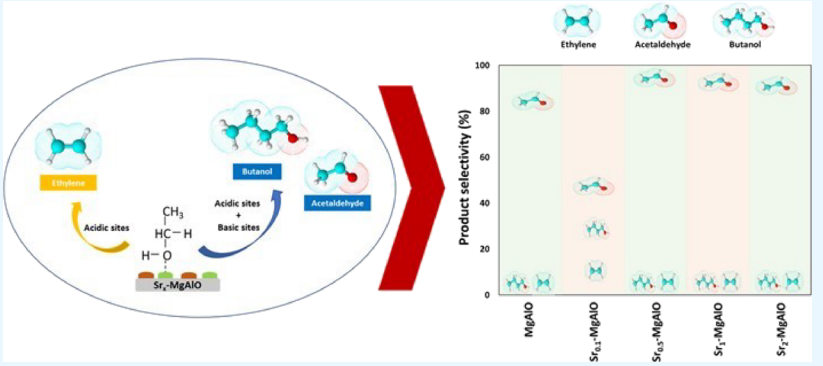

ABSTRACT: The aim of this research was to examine the effect of strontium content in the MgAlO catalyst for the catalytic ethanol reaction on the product distribution. The structure of the catalysts and the actual amount of strontium on the catalysts were verified using XRD and ICP techniques, respectively. The acid and basic strength characteristics of catalysts were examined using NH_3-TPD and CO_2-TPD techniques, respectively. The strontium content was found to influence the textural properties and the acidic and basic characteristics of the catalysts, leading to differences in product selectivity and ethanol conversion. The MgAlO catalyst with 1.9 wt % strontium provided the maximum ethylene and butanol selectivity, probably due to the presence of appropriate medium acidic and strong basic sites. All catalysts can efficiently produce ethylene by a dehydration reaction and acetaldehyde by a dehydrogenation reaction. Acetaldehyde selectivity was dominant with increased strontium loading.

1. INTRODUCTION

There is currently a tendency toward environment preservation that necessitates the development of new biodegradable products created from biological molecules.[1] It benefits in fewer waste and pollution in the long run. As a result, bioethanol is attentively used as a crucial precursor for the production of a variety of high-value biochemicals and fuels. Bioethanol is ethanol derived from agricultural products or agricultural wastes through biological processes. Several reactions of ethanol can synthesize a variety of organic chemicals, namely, acetaldehyde, ethylene, diethyl ether, butanol, etc.[2,3] Catalytic dehydration of ethanol at high and low reaction temperatures yields ethylene and diethyl ether, respectively.[4−6] This reaction requires an acidic catalyst; the hydroxyl group of an ethanol molecule is protonated by an acid active site in the catalyst, leading to the formation of ethylene and diethyl ether. Ethanol dehydrogenation produces acetaldehyde, which prefers a basic catalyst. Acetaldehyde is utilized as an intermediate in the production of important chemicals such ethyl acetate.[7,8] Butanol is also produced by direct dimerization of two molecules of ethanol and/or by Guerbet reaction. Dehydrogenation of a primary ethanol to acetaldehyde, aldol condensation of acetaldehyde to acetaldol, dehydration of acetaldol to crotonaldehyde, and finally hydrogenation of crotonaldehyde to form butanol are all parts of the Guerbet reaction.[9,10] These are fundamental chemicals in a wide range of industries, namely, food, beverage, cosmetics, petrochemicals, and others. Thus, developing technologies will indeed be both safe to use and environmentally friendly when all substances are manufactured from bio-based raw materials.

The type of catalyst has the greatest impact on the product formation of the ethanol reaction. The properties of different types of catalysts vary, especially their acidic and basic features. In previous research on ethanol reactions, heterogeneous catalysts such as metal oxides,[11,12] zeolite,[13] hydroxyapatites (HAP),[14−16] and activated carbon catalysts[17,18] were investigated. The performance of the Mg−Al mixed oxide catalyst

Received: May 28, 2023
Accepted: August 15, 2023
Published: August 29, 2023

(MgAlO) produced by calcination of Mg−Al layered double hydroxide precursors (Mg−Al LDH) in ethanol conversion was also studied. The Mg−Al LDH catalyst has a double layer of Mg and Al metal cations with an anion structure between them. The bifunctional cation and anion are both present in this catalyst structure. However, MgAlO has an unstable structure. It can revert to an LDH structure when exposed to moisture after calcination due to its structural memory property.[19] The MgAlO catalyst is unique in that it does not require a reducing procedure to generate an active site for accelerating ethanol conversions, thus consuming less energy and preparation time.

Metals were added to MgAlO catalysts to improve the efficiency of ethanol conversion into higher-value products. The acidic and basic properties of MgAlO catalysts were altered by the addition of metals. Moreover, the type of metal added to catalysts is related to product selectivity. Pd, Ag, Mn, Fe, Cu, Sm, and Yb were added to the MgAl mixed oxide catalyst derived from LDH precursors.[20] The Pd-modified MgAlO had the highest butanol conversion and butanol yield due to its high basic site content and optimum acidic/basic site ratio. Pd-MgAlO had very high basic sites but less than Sm-MgAlO, while Pd-MgAlO had less acidity than Fe-MgAlO, Mn-MgAlO, Ag-MgAlO, and Cu-MgAlO. However, it had the best catalytic activity. It is possible that the appropriate catalyst should have an optimum basic/acidic ratio for the Guerbet reaction. Furthermore, the addition of a second metal to a mixed oxide catalyst can enhance the butanol production performance. Palladium or indium metal was added to the CuMgAlO catalyst.[21] The Pd-CuMgAlO and In-CuMgAlO catalysts had significant hydrogen transfer and basic site content, which improved the catalytic activity of the MgAlO catalyst. Palladium and indium metal on catalysts could help in reducing the desorption temperature for strong basic and strong acidic sites, leading butanol to be produced at a lower temperature than pure CuMgAlO. The Sr-HAP catalysts promoted the hydrogen transfer reaction in butanol synthesis and the aldol condensation of acetaldehyde with remarkable selectivity. It also prevented coke formation in the reaction. The metal molar ratios in the structure of the strontium phosphate hydroxyapatite catalyst were also studied.[22−24] The Sr/P molar ratios influenced the catalytic activity of the hydroxyapatite catalyst and selectivity. Catalytic activity and 1-butanol selectivity were better in Sr-HAP catalysts with larger Sr/P molar ratios. As the Sr-P molar ratio increased, the density of the relatively strong acidic and basic sites of the catalyst increased with the density of the basic site being much higher than that of the acidic site. High acidity and basicity catalysts do not always result in high conversion and product selectivity, while low acidity and basicity catalysts do not always result in low conversion and product selectivity, but an optimum ratio of acidic and basic functions is necessary for the reaction.[25−27] The number of weak, medium, and strong acidic and basic sites correlated with product selectivity as well.[28,29]

The aim of this research is to investigate how strontium loading on a MgAlO catalyst affects catalytic performance and product selectivity in the ethanol reaction. The influence of strontium content on the efficiency of the MgAlO catalyst was also studied. The strontium-containing catalysts were synthesized using an incipient wetness impregnation method and characterized using various techniques. The reaction was examined in a gas phase continuous fixed-bed microreactor.

2. EXPERIMENTAL SECTION

2.1. Catalyst Preparation. All of the starting reagents including $Mg(NO_3)_2{\cdot}6H_2O$, $Al(NO_3)_3{\cdot}9H_2O$, $Sr(NO_3)_2$, NaOH, and Na_2CO_3 were purchased from Sigma-Aldrich Chemical Company, Inc. The magnesium aluminum mixed oxide catalyst (MgAlO) was synthesized by a coprecipitation method following a previously reported procedure.[30] The following procedure was started by coprecipitating $Mg(NO_3)_2{\cdot}6H_2O$ and $Al(NO_3)_3{\cdot}9H_2O$ in DI water, then slowly dropping the coprecipitation solution into a sodium solution of NaOH and Na_2CO_3 with a pH control of 10, and keeping it at 65 °C for 18 h to obtain the mixture solution in hydrotalcite structure form. The MgAl layered double hydroxide (MgAl-LDH) was obtained after washing the hydrotalcite solution with DI water and drying it. The resultant solid was further calcined at 450 °C for 6 h to yield MgAl mixed oxide. Finally, strontium-supported MgAlO catalysts were prepared by an incipient wetness impregnation method with varying strontium per MgAlO molar ratio and calcined at 450 °C for 6 h. The catalysts were labeled Sr_x-MgAlO, where x represents the molar ratio of strontium to MgAlO.

2.2. Catalyst Characterization. X-ray diffraction (XRD) was used to confirm the structure of catalysts. XRD was carried out at 2θ in a range of 10 to 80° with a scan speed of 0.5 s/step. A N_2 physisorption method was performed to determine the BET surface area, pore volume, and pore size of catalysts. The catalysts were degassed at 150 °C for 3 h before analysis. The basic and acidic characteristics of catalysts were measured by temperature-programed desorption (TPD) on a Micromeritics Chemisorb 2750 automated system using CO_2 and NH_3 as desorption gas, respectively. The catalyst was preheated at 450 °C for 1 h under helium to eliminate moisture and impurities, and then, CO_2 or NH_3 gas was supplied until saturation was achieved. TPD was started at a heating rate of 10 °C/min from 30 to 800 °C. The basic and acidic characteristics of catalysts were computed and evaluated using the results of CO_2-TPD and NH_3-TPD analysis. Thermogravimetric analysis (TGA) with an STD analyzer model Q600 was conducted in air at a heating rate of 10 °C/min to examine the thermal decomposition of catalysts. The thermal behaviors of catalysts were studied at temperatures ranging from ambient temperature to 1000 °C.

2.3. Ethanol Reaction. The ethanol reaction was performed in a fixed-bed continuous flow microreactor. Typically, 0.1 g of Sr_x-MgAlO catalysts was packed on the quartz wool in the middle of the reactor, preheated at 200 °C for 1 h in nitrogen at a flow rate of 900 mL/h, and then cooled down to the specified reaction temperature before catalytic study. The reaction was operated at temperatures ranging from 200 to 400 °C under atmospheric pressure at a weight hourly space velocity (WHSV) constant of 3.1 h^{-1}. The products were collected at the sampling point after samples were out of the reactor, and the products were analyzed by gas chromatography with a flame ionization detector (GC-FID) using a DB-5 capillary column. The following equations were used to calculate the ethanol conversion, percentage selectivity of products, and percentage yields of products:

Ethanol conversion

$$X(\%) = \frac{n_{\text{ethanol}}(\text{in}) - n_{\text{ethanol}}(\text{out})}{n_{\text{ethanol}}(\text{in})} \times 100 \quad (1)$$

https://doi.org/10.1021/acsomega.3c03752
ACS Omega 2023, 8, 32775−32783

Percentage selectivity of products

$$S_i(\%) = \frac{n_i}{\sum n_i} \times 100 \quad (2)$$

Percentage yields of products

$$Y_i(\%) = \frac{X_{\text{ethanol}} \times S_i}{100} \quad (3)$$

where n_i is the mole of product and $\sum n_i$ is the total moles of products based on carbon balance.

3. RESULTS AND DISCUSSION

3.1. Catalyst Characterizations. The catalysts featured MgAlO-based structures with differences in the amount of strontium impregnated into particles. The structure of each catalyst was determined using the XRD technique, as shown in Figure 1. The significant broad peaks at approximately 43 and

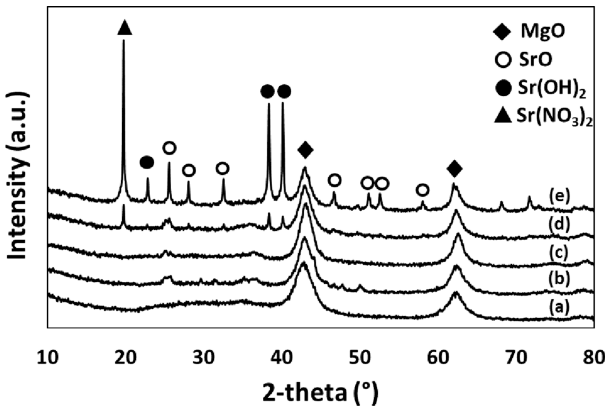

Figure 1. XRD patterns of catalysts: (a) MgAlO, (b) $Sr_{0.1}$-MgAlO, (c) $Sr_{0.5}$-MgAlO, (d) Sr_1-MgAlO, and (e) Sr_2-MgAlO.

62° in the XRD pattern of the MgAlO catalyst without strontium in Figure 1a were ascribed to a periclase MgO phase,[30,31] which was formed during the calcination of MgAl-LDH.[32−34] The MgO phase was also seen in the other catalysts impregnated with strontium molecules. However, the Al_2O_3 phase was not observed because the MgO phase is more crystalline than Al_2O_3, leading to a reduction in the peak of Al_2O_3 and resulting in a peak overlap.[35−37] The peak of strontium oxide (SrO) and strontium hydroxide [$Sr(OH_2)$] was clearly detected when the molar ratio of strontium was increased. Since the small strontium content could be well dispersed over the catalyst surface, the XRD patterns of $Sr_{0.1}$-MgAlO and $Sr_{0.5}$-MgAlO catalysts in Figure 1b,c, respectively, revealed a slight peak of strontium. The peaks of strontium compounds were clearly observed in the XRD pattern of the Sr_2-MgAlO catalyst (Figure 1d). The strontium oxide (SrO) phase formed during the calcination of MgAlO impregnated with strontium nitrate [$Sr(NO_3)_2$] at 450 °C was associated to the sharp diffraction peaks on Bragg angles 2θ of 25.6, 28.1, 32.5, 46.7, 51.1, 52.3, and 58.0°.[38−40] The presence of strontium hydroxide [$Sr(OH)_2$] was suggested by the characteristic peaks at 22.8, 38.3, and 40.1°, which seemed possibly owing to hydration.[38,39] The sharp diffraction peaks of both SrO and $Sr(OH)_2$ in the Sr_2-MgAlO catalyst indicated the formation of high crystallinity. However, the addition of a large amount of strontium led to the appearance of a $Sr(NO_3)_2$ phase at 19.8°.[41] It means that when a larger concentration of $Sr(NO_3)_2$ was employed as a precursor, the calcination of the nitrate compound was incomplete. The findings indicate that the mixed oxide structure was verified in all of the catalysts. Moreover, the morphology of all catalysts was investigated by the SEM technique, and the SEM images of Sr_x-MgAlO catalysts are shown in Figure S1 in the Supporting Information. The SEM images indicated that the addition of high weight percent of strontium molecules caused the agglomeration of particles.

The nitrogen adsorption−desorption isotherms of the catalysts are shown in Figure 2. According to IUPAC, the

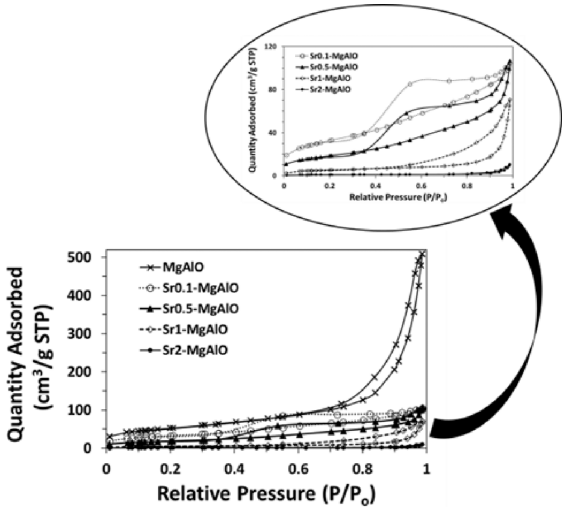

Figure 2. N_2 adsorption−desorption isotherms of catalysts.

observed isotherm diagrams are a type IV isotherm, which is related with the presence of mesoporous structures.[42,43] The curves of the adsorption−desorption isotherm exhibited a hysteresis loop at high relative pressures. However, the desorption lines of each catalyst varied, bringing about differences in hysteresis loops, and the shape of which has been associated with specific pore structures of the catalysts. The MgAlO catalyst exhibited a type H3 hysteresis loop that was coupled with plate-like particle aggregates, resulting in slit-shaped pores.[44] The $Sr_{0.1}$-MgAlO and $Sr_{0.5}$-MgAlO loop displayed a perpendicular desorption branch, which is a typical feature of type H2a loops. This is due to pore blockage in a restricted range of pore necks. The hysteresis loops of Sr_1-MgAlO and Sr_2-MgAlO were comparable to type H2b also involved in the pore blocking effect, but the size variation of neck widths had become significantly greater.[43,45] The isotherm shape of the catalyst with the highest quantity of strontium resembled the smallest loop, indicating that the interaction between the adsorbent and adsorbate was rather weak and that the adsorbed molecules gathered on the surface of the low porosity catalyst. So, when more strontium was loaded on the catalyst, there was an increase in the pore blockage. The results are in accordance with chemical composition, specific surface area, pore size, and pore volume of the catalyst, as presented in Table 1.

The molar ratio of strontium was modified from 0.1, 0.5, 1, and 2 in catalysts with the same Mg and Al molar ratio of 5:1. ICP analysis confirmed the actual concentration of strontium on the catalysts, and the actual weight percentage of components in the catalysts was calculated and is given in Table 1. With additional strontium in MgAlO, the BET surface

https://doi.org/10.1021/acsomega.3c03752
ACS Omega 2023, 8, 32775−32783

Table 1. Chemical and Textural Properties of Catalysts

	concentration of elements (mg/L)[a]			weight[a] (%)					
catalyst	Mg	Al	Sr	Mg	Al	Sr	BET surface area (m^2/g)	average pore volume (cm^3/g)	average pore size (nm)
MgAlO	5.06	1.00		83.4	16.6		189.7	0.79	13.4
$Sr_{0.1}$-MgAlO	6.35	1.28	0.15	81.6	16.5	1.9	118.3	0.17	3.6
$Sr_{0.5}$-MgAlO	6.76	1.56	0.64	75.4	17.4	7.2	67.5	0.17	4.7
Sr_1-MgAlO	6.78	1.43	1.16	72.4	15.2	12.4	50.5	0.14	10.4
Sr_2-MgAlO	6.45	1.36	2.21	64.3	13.6	22.1	29.6	0.10	37.0

[a]Concentration and weight percent of elements in the catalysts were determined by the ICP technique.

Table 2. Amounts of Basic Sites and Acidic Sites Determined by the Temperature-Programmed Desorption Technique

	basicity (μmol/g)				acidity (μmol/g)				
catalysts	W	M	S	total	W	M	S	total	total basicity/total acidity ratio
MgAlO	117	16	89	222	191	594	882	1667	0.13
$Sr_{0.1}$-MgAlO	16	19	74	109	268	34	1030	1332	0.08
$Sr_{0.5}$-MgAlO	5	19	121	145	209	0	1477	1686	0.09
Sr_1-MgAlO	0	3	112	115	274	0	2296	2570	0.05
Sr_2-MgAlO	0	0	191	191	144	0	2966	3110	0.06

area and average pore volume of catalysts would be reduced. The highest surface area was 189.7 m^2/g in MgAlO, while Sr_2-MgAlO had only 29.6 m^2/g. These results were probably caused by the large size of the strontium molecule blocking pores and/or inducing cavitation in the catalyst.[46] The average pore size of catalyst was also reduced when catalysts were impregnated with strontium. However, the pore size of Sr_2-MgAlO was considerably enlarged after impregnation with a strontium molar ratio of 2 and calcination at 450 °C due to the collapse of the MgAlO framework.[40]

The acidic and basic sites of the catalyst have a significant impact on the catalytic activity of the catalyst for ethanol conversion. The acidity and basicity of the catalysts are shown in Table 2 as determined with the NH_3-TPD and CO_2-TPD techniques, respectively. The acidic and basic sites of catalysts were resolved from room temperature until 800 °C, and they were divided into three main types based on desorption temperature: weak sites with a desorption temperature less than 250 °C, moderate sites with a desorption temperature between 250 and 400 °C, and strong sites with desorption higher than 400 °C. MgAlO has a total basicity of 222 μmol/g, whereas other Sr-impregnated catalysts have a lower total basicity. Normally, isolated O^{2-}, Mg^{2+}-O^{2-} pairings, and hydroxyl groups (−OH) are three types of basic sites found in Mg_yAlO_x catalysts. Strong basic sites are commonly considered the isolated O^{2-} of MgO crystallites, but the addition of Al increases the relative concentrations of other weak basic sites and the acidic site density.[7,47] The metal addition alters the density of surface acidic and basic sites along with the strength distribution of Mg_yAlO_x catalysts. The introduction of strontium reduced the total basicity of Sr_x-MgAlO catalysts, probably due to strontium compounds covering the basic sites of MgAlO.[7]

The CO_2-TPD analysis showed that when the strontium content in the Sr-impregnated catalyst was increased, weak basic sites drastically decreased. The medium basic sites were slightly modified by Sr-impregnated catalysts with molar ratios of 0.1 and 0.5, but they were dramatically decreased by higher strontium loading. On the other hand, strong basic sites were increased as a result of SrO providing strong basicity.[38,40] Only strong basic sites were found on the catalyst with the highest strontium content.

For the acidic property of catalysts, the weak acidic sites were slightly modified by increasing the strontium content on catalysts. However, for all Sr-impregnated catalysts, the medium acidic sites were considerably reduced, whereas the strong acidic sites and total acidity were enhanced. With the exception of $Sr_{0.1}$-MgAlO, no medium acidic sites were found on the Sr_x-MgAlO catalysts. Thus, strontium addition influenced the basic and acidic properties of catalysts, particularly an increase in strong acidic and basic sites. Figure 3 also depicts the NH_3 desorption and CO_2 desorption profile of all catalysts. The profiles that correspond to the acidity and basicity of catalysts are shown in Table 2. When strontium was added to the MgAlO catalyst, the NH_3 desorption and CO_2 desorption profiles at the strong acidic and basic peak shifted to a lower temperature. This might increase the product selectivity at lower temperatures.[21]

3.2. Catalytic Ethanol Reaction. To study the effect of MgAlO catalysts with various strontium contents prepared by impregnation and calcination without the reducing step, the ethanol reaction was carried out at a reaction temperature ranging from 200 to 400 °C under atmospheric pressure. It was evaluated by determining the ethanol conversion, product selectivity, and catalyst stability. The ethanol conversion from various catalysts at different reaction temperatures is shown in Figure 4. The ethanol conversion was promoted by increasing the reaction temperature. The MgAlO catalyst converted more ethanol than all of the Sr_x-MgAlO catalysts because the addition of strontium to the catalyst changed its structure. Strontium molecules clogged the pores and collapsed the pore structure, resulting in a lower pore volume and surface area as well as a larger pore width. At a constant reaction temperature, the ethanol conversion of all catalysts was consistent with their acidic and basic properties. When the ratio of total basic sites to total acidic sites was increased, as indicated in Table 2, ethanol conversion was increased.

Ethylene, acetaldehyde, diethyl ether, butanol, ethyl acetate, acetic acid, and others such as acetaldol, crotonaldehyde, and butanal are among the results of the ethanol conversion through a multistep reaction using MgAlO and Sr_x-MgAlO as a

https://doi.org/10.1021/acsomega.3c03752
ACS Omega 2023, 8, 32775−32783

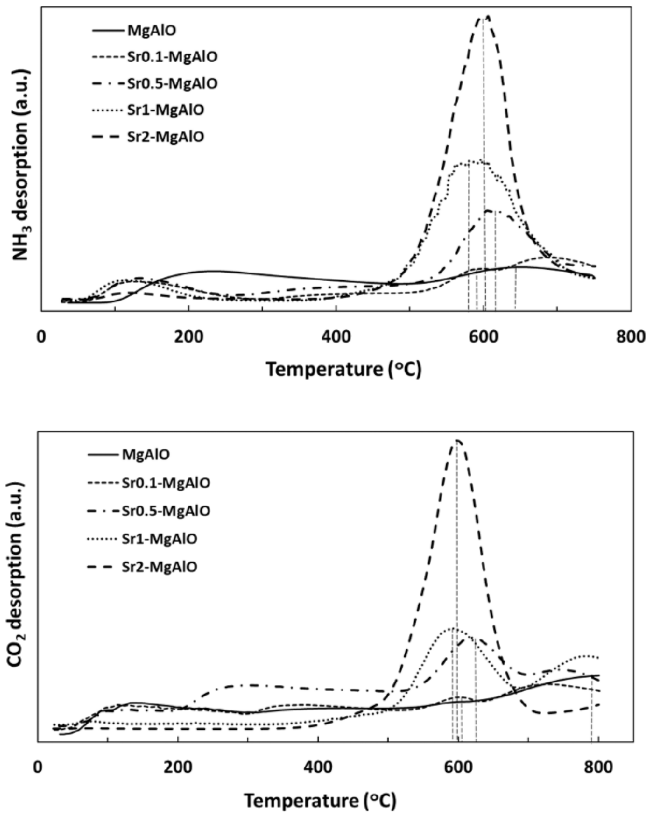

Figure 3. NH_3-TPD and CO_2-TPD analysis of all catalysts.

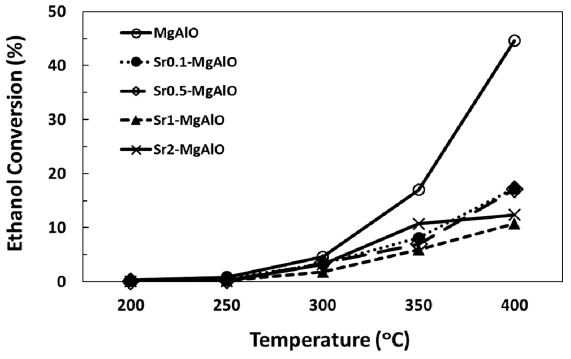

Figure 4. Ethanol conversion over MgAlO and Sr_x-MgAlO with different strontium contents.

catalyst. The product yield and selectivity over MgAlO and MgAlO with varying strontium molar ratio at constant ethanol and inert gas flow rates are presented in Figure 5 and Table 3, respectively. The high ethylene yield was obtained with MgAlO, $Sr_{0.1}$-MgAlO, and $Sr_{0.5}$-MgAlO. However, a greater strontium molar ratio led to a lower ethylene yield. The highest diethyl ether was produced by the MgAlO catalyst. When the strontium loading on the MgAlO catalyst was increased, the yield of diethyl ether was significantly decreased until it disappeared at the highest strontium content. In fact, the acid strength and type of acid site mainly influence the activity of catalyst in ethanol dehydration to ethylene and ether. Dehydration of ethanol to ethylene generally necessitates a large number of weak acidic sites and a small number of medium strong acidic sites.[48,49] The best yield of ethyl acetate was obtained with $Sr_{0.1}$-MgAlO, but ethyl acetate was not detected at a higher strontium content. Acidic site properties

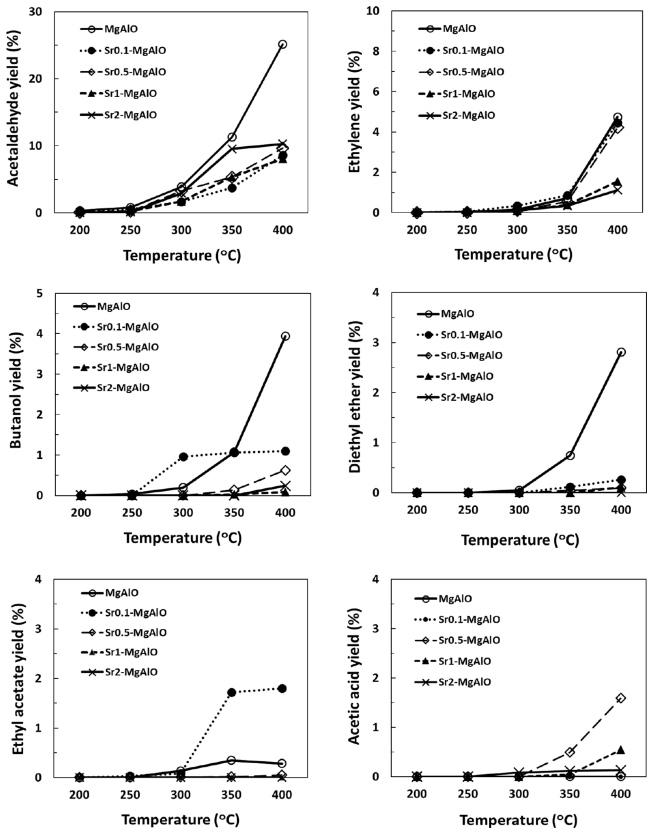

Figure 5. Product yields over MgAlO and Sr_x-MgAlO with different strontium contents.

are required for the formation of ethylene, diethyl ether, and ethyl acetate. The NH_3-TPD results suggest that increasing the strontium content resulted in the absence of the medium acidic site. On the other hand, the strong acidic site was significantly increased. The excessive divergence of the weak, medium, and strong acidic sites prohibited the formation of products.

Acetaldehyde was the predominant product on all of the catalysts with the highest yield and selectivity, and it can be produced at temperatures as low as 200 °C. The yield of acetaldehyde increased as the reaction temperature increased. In the case of strontium-modified catalysts, increasing the strontium molar ratio increased acetaldehyde yield, possibly due to increased strong basic sites. As shown in Figure 5, the highest acetaldehyde yield was obtained with Sr_2-MgAlO at a reaction temperature of 400 °C. Di Cosimo et al. reported that ethanol dehydration to acetaldehyde required both weak acidic and strong basic sites.[47] However, an improper ratio of acidic to basic sites on the catalyst may cause the accumulation of acetaldehyde, which may prevent the production of other products. The butanol production using MgAlO and Sr-MgAlO catalysts requires a reaction temperature greater than 200 °C. The butanol yield of the MgAlO catalyst was comparatively higher than those of all Sr-MgAlO catalyzed reactions at temperatures over 350 °C. Meanwhile, $Sr_{0.1}$-MgAlO produced the best butanol yield at temperatures lower than 350 °C. However, the butanol yield dropped as the amount of strontium on MgAlO increased due to decreased ethanol conversion. The addition of a small amount of strontium to MgAlO could boost butanol production at lower reaction temperatures by decreasing the temperature of the desorption peaks for strong acidic and basic sites. This

https://doi.org/10.1021/acsomega.3c03752
ACS Omega 2023, 8, 32775−32783

Table 3. Ethanol Conversion and Product Selectivity from Various Catalysts as a Function of Temperature

			product selectivity (%)						
catalysts	Temp. (°C)	ethanol conversion (%)	ethylene	acetaldehyde	diethyl ether	ethyl acetate	acetic acid	butanol	other
MgAlO	200	0.29	0	100.00	0	0	0	0	0
	250	0.83	3.54	92.60	0	0	0	3.85	0
	300	4.58	3.12	84.68	0.98	2.92	0	4.21	5.48
	350	16.97	4.19	66.66	4.37	2.04	0	6.31	16.42
	400	44.56	10.64	56.39	6.30	0.63	0	8.84	17.46
$Sr_{0.1}$-MgAlO	200	0.20	0	100.00	0	0	0	0	0
	250	0.63	8.76	86.39	0	4.85	0	0	0
	300	3.30	10.09	49.21	0	2.39	0	29.09	9.22
	350	8.16	10.55	46.00	1.39	21.10	0	12.97	8.00
	400	17.23	25.81	49.81	1.50	10.46	0	6.37	6.05
$Sr_{0.5}$-MgAlO	200	0.05	0	100.00	0	0	0	0	0
	250	0.25	4.68	95.32	0	0	0	0	0
	300	3.43	3.19	95.41	0	0.24	0	0	1.16
	350	6.94	7.74	76.38	0.59	0.23	7.12	1.95	5.98
	400	17.09	24.67	56.48	0.55	0.30	9.31	3.65	5.04
Sr_1-MgAlO	200	0.14	0	100.00	0	0	0	0	0
	250	0.25	9.83	90.17	0	0	0	0	0
	300	1.85	4.98	93.81	0	0	0	0	1.21
	350	5.91	6.41	90.29	0	0	0.79	0.44	2.07
	400	10.78	14.26	75.05	0.98	0	5.07	0.74	3.89
Sr_2-MgAlO	200	0.03	0	100.00	0	0	0	0	0
	250	0.11	0	100.00	0	0	0	0	0
	300	3.18	3.03	91.92	0	0	2.73	0	2.31
	350	10.70	3.12	89.03	0	0	1.07	0	6.78
	400	12.38	9.00	83.01	0	0	1.06	1.93	5.00

corresponds to the $Sr_{0.1}$-MgAlO catalyst having the maximum butanol and ethylene selectivity at lower temperatures compared to the MgAlO catalyst. Furthermore, ethyl acetate was generated at a lower temperature than when the MgAlO catalyst was used. It may be stated that the introduction of strontium to MgAlO catalysts plays an important role in the ethanol transformation by accelerating the low-temperature reaction.[21]

As previously noted, the product formation depends on the acidic and basic characteristics of the catalyst. In part of the multistep ethanol conversion to butanol, the strong basic sites promote the aldol condensation pathway of acetaldehyde molecules, and the medium acidic sites probably promote the dehydration step.[30] Although the acetaldehyde selectivity was increased when the strontium molar ratio was raised from 0.1 to 2, the butanol selectivity was decreased. This might be because increasing the strontium molar ratio strengthened the strong basic sites of the catalysts but decreased the medium acidic sites. Sr_x-MgAlO catalysts with small amounts of strontium were better suited to the acidity and basicity of the catalyst for butanol generation. $Sr_{0.1}$-MgAlO showed the highest butanol selectivity of 29% at 300 °C. High strontium on the catalysts decreased ethanol conversion and butanol selectivity by causing an imbalance of medium acid and strong basic sites as well as a drastic reduction in surface area and pore volume. These catalysts mostly exhibited high amounts of strong acidic and basic sites with no medium acidic sites. In contrast, the strong acidic and basic sites most likely produced acetic acid from ethanol.

However, the product selectivity of each product was analyzed and compared with changing of basicity and acidity properties of the catalyst when the strontium atom was loaded on the MgAlO catalyst. It was possible to predict how basicity and acidity properties of catalysts were suitable for each product production. A suitable catalyst for ethylene production should have acidic sites, especially weak and strong acidic sites. Diethyl ether and ethyl acetate also required extremely acidic sites, particularly medium acidic sites. Since medium acidic sites were absent when strontium was loaded on the MgAlO catalyst in molar ratios of 0.5, 1, and 2, diethyl ether and ethyl acetate were not produced. The MgAlO catalyst had the highest acetaldehyde selectivity, but the acetaldehyde selectivity was decreased with strontium loading on the MgAlO catalyst because weak basic and medium acidic sites were decreased and strong basic and strong acidic sites were increased. Thus, acetaldehyde required weak and strong basic sites and medium and strong acidic sites. For butanol, the transformation of ethanol to butanol was a multistep reaction consisting of the aldol condensation that required strong basic sites and the dehydration step that required medium acidic sites.[30] The catalytic ethanol reaction test showed that the result, as shown in Table 3, is related to the amounts of the basic and acidic sites determined by the TPD technique. For this result, the suitable catalyst for butanol production included medium and strong basic sites and all weak, medium, and strong acidic sites. Although the Sr_xMgAlO catalyst did not contain medium acidic sites, it was still capable to produce butanol at high temperatures. In addition, the formation of acetic acid needed strong basic and strong acidic sites.

Carbon deposition on spent catalysts was investigated by thermogravimetric analysis at room temperature up to 1000 °C in an ambient atmosphere. The percentage of weight loss and percentage of derivative weight for all spent catalysts are shown in Figure 6. The quantity of carbon deposition on catalysts would be represented by the percentage of weight loss. The elimination of moisture on catalysts caused weight loss in the

https://doi.org/10.1021/acsomega.3c03752
ACS Omega 2023, 8, 32775−32783

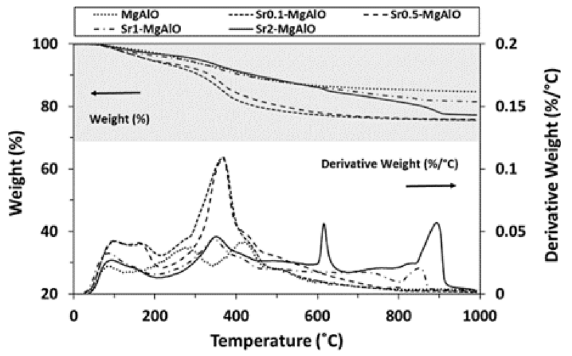

Figure 6. Thermogravimetric analysis of spent catalysts: weight (%) and derivative weight (%/°C).

first region at room temperature up to 200 °C.[50] Calcination of the hydrotalcite structure produced the metal mixed oxide structure. However, moisture can cause its structure to revert to hydrotalcite. The weight loss at temperatures ranging from 200 to 450 °C was induced by dihydroxylation and decarbonation of the hydrotalcite structure, which resulted in the formation of metal oxide particles.[50,51] The decoking process is divided into three regions with temperatures ranging from 200 to 1000 °C.[52] The first region of decoking was soft coke at temperatures ranging from 200 to 400 °C, while the second region was hard coke at temperatures ranging from 400 to 600 °C. The last region, which ranges from 650 to 1000 °C, was referred to as carbon deposition in catalyst pores. At temperatures ranging from 200 to 450 °C, the percentages of weight loss on MgAlO, $Sr_{0.1}$-MgAlO, $Sr_{0.5}$-MgAlO, Sr_1-MgAlO, and Sr_2-MgAlO were found to be around 8.1, 15.4, 13.3, 7.3, and 7.2%, respectively. During this temperature range, $Sr_{0.1}$-MgAlO exhibited the highest percentage of weight loss. This is attributed to both the transformation of the hydrotalcite structure to metal oxide and decoking of soft coke. The soft coke can be easily removed at low temperatures. The Sr_2-MgAlO catalyst shows the lowest percentage of weight loss at temperatures ranging from 200 to 450 °C but the highest weight loss at temperatures ranging from 400 to 600 °C and 650 to 1000 °C. Despite having the lowest percentage of ethanol conversion due to pore blocking in the catalyst structure and the unsuitability of the basic−acidic sites, Sr_2-MgAlO from 400 to 1000 °C might be ascribed to the elimination of the residual $Sr(NO_3)_2$, as proven by XRD results, as well as the loss of coke deposits in pores. The occurrence of more hard coke was attributed to Sr_2-MgAlO possessing the strongest acidic and basic sites. This finding differs from that of Ogo et al. who discovered that the presence of strontium on the hydroxyapatite catalyst benefited the prevention of coke formation during the hydrogen transfer conversion of 2-buten-1-ol to butanol.[22] The results suggest that butanol may be produced over the Sr-MgAlO catalysts in various routes. When a proper quantity of strontium was loaded onto the catalyst, it had good activity for the ethanol reaction to butanol and reduced hard coke formation.

4. CONCLUSIONS

This research investigated the influence of strontium content loading on MgAlO catalysts during ethanol conversion in a continuous flow fixed-bed reactor with the reaction temperature range of 200 to 400 °C. The strontium content was discovered to have effects on the textural and chemical properties of the catalysts. As the quantity of strontium increased, the surface area and porosity of the catalysts decreased significantly due to pore blockage while the pore size increased. Increased strontium lead to an increase in the strong acidic and basic sites but caused a considerable drop in the weak basic and medium acidic sites, causing lowering ethanol conversion and ethylene and butanol selectivity. However, a higher strontium content improved acetaldehyde selectivity. With increasing strontium, total acidity was increased but total basicity was decreased. All of the catalysts can be used for the production of acetaldehyde through a dehydrogenation reaction and ethylene through dehydration reaction. The MgAlO catalyst produced the highest acetaldehyde yield at a reaction temperature of 400 °C. $Sr_{0.1}$-MgAlO showed the highest ethylene selectivity at 400 °C and the highest butanol selectivity at 300 °C. Diethyl ether, ethyl acetate, acetic acid, and other C4 compounds were such little produced.

■ ASSOCIATED CONTENT

Supporting Information

The Supporting Information is available free of charge at https://pubs.acs.org/doi/10.1021/acsomega.3c03752.

SEM images of the MgAlO, $Sr_{0.1}$-MgAlO, $Sr_{0.5}$-MgAlO, Sr_1-MgAlO, and Sr_2-MgAlO catalysts (PDF)

■ AUTHOR INFORMATION

Corresponding Author

Bunjerd Jongsomjit − *Center of Excellence on Catalysis and Catalytic Reaction Engineering, Department of Chemical Engineering, Faculty of Engineering and Bio-Circular-Green-Economy Technology & Engineering Center (BCGeTEC), Department of Chemical Engineering, Faculty of Engineering, Chulalongkorn University, Bangkok 10330, Thailand;* orcid.org/0000-0002-9558-9190; Email: bunjerd.j@chula.ac.th

Authors

Patchaporn Seekhiaw − *Center of Excellence on Catalysis and Catalytic Reaction Engineering, Department of Chemical Engineering, Faculty of Engineering and Bio-Circular-Green-Economy Technology & Engineering Center (BCGeTEC), Department of Chemical Engineering, Faculty of Engineering, Chulalongkorn University, Bangkok 10330, Thailand*

Sasiradee Jantasee − *Department of Chemical and Materials Engineering, Faculty of Engineering, Rajamangala University of Technology Thanyaburi, Pathum Thani 12110, Thailand*

Piyasan Praserthdam − *Center of Excellence on Catalysis and Catalytic Reaction Engineering, Department of Chemical Engineering, Faculty of Engineering and Bio-Circular-Green-Economy Technology & Engineering Center (BCGeTEC), Department of Chemical Engineering, Faculty of Engineering, Chulalongkorn University, Bangkok 10330, Thailand;* orcid.org/0000-0001-8021-2115

Complete contact information is available at: https://pubs.acs.org/10.1021/acsomega.3c03752

Notes

The authors declare no competing financial interest.

■ ACKNOWLEDGMENTS

This research is funded by Thailand Science Research and Innovation Fund Chulalongkorn University (IND66210016),

the Graduate School of Chulalongkorn University, and CATREAC industrial project. This research and innovation activity is also funded by National Research Council of Thailand (NRCT).

REFERENCES

(1) Rathore, A. S.; Singh, A. Biomass to fuels and chemicals: A review of enabling processes and technologies. *J. Chem. Technol. Biotechnol.* **2022**, *97*, 597−607.
(2) Mück, J.; Kocík, J.; Frolich, K.; Šimek, J.; Michálková, M.; Hájek, M. Transition Metal-Promoted Mg-Fe Mixed Oxides for Conversion of Ethanol to Valuable Products. *ACS Omega* **2023**, *8*, 19374−19384.
(3) Liu, Q.; Zhou, H.; Jia, Z. Hydrogen Production by Ethanol Reforming on Supported Ni-Cu Catalysts. *ACS Omega* **2022**, *7*, 4577−4584.
(4) Varisli, D.; Dogu, T.; Dogu, G. Ethylene and diethyl-ether production by dehydration reaction of ethanol over different heteropolyacid catalysts. *Chem. Eng. Sci.* **2007**, *62*, 5349−5352.
(5) Bokade, V. V.; Yadav, G. D. Heteropolyacid supported on montmorillonite catalyst for dehydration of dilute bio-ethanol. *Appl. Clay Sci.* **2011**, *53*, 263−271.
(6) Autthanit, C.; Likitpiriya, N.; Praserthdam, P.; Jongsomjit, B. Development of a New Ternary $Al_{(2)}O_{(3)}$-HAP-Pd Catalyst for Diethyl Ether and Ethylene Production Using the Preferential Dehydration of Ethanol. *ACS Omega* **2021**, *6*, 19911−19923.
(7) Pang, J.; Zheng, M.; He, L.; Li, L.; Pan, X.; Wang, A.; Wang, X.; Zhang, T. Upgrading ethanol to n-butanol over highly dispersed Ni−MgAlO catalysts. *J. Catal.* **2016**, *344*, 184−193.
(8) Preedavijitkul, S.; Autthanit, C.; Praserthdam, P.; Jongsomjit, B. Role of Cr on Cu-Cr catalyst via direct ethanol dehydrogenation to ethyl acetate. *J. Envi. Chem. Eng.* **2022**, *10*, No. 107542.
(9) Silvester, L.; Lamonier, J.-F.; Lamonier, C.; Capron, M.; Vannier, R.-N.; Mamede, A.-S.; Dumeignil, F. Guerbet Reaction over Strontium-Substituted Hydroxyapatite Catalysts Prepared at Various (Ca+Sr)/P Ratios. *ChemCatChem* **2017**, *9*, 2250−2261.
(10) Wu, X.; Fang, G.; Tong, Y.; Jiang, D.; Liang, Z.; Leng, W.; Liu, L.; Tu, P.; Wang, H.; Ni, J.; Li, X. Catalytic Upgrading of Ethanol to n-Butanol: Progress in Catalyst Development. *ChemSusChem* **2018**, *11*, 71−85.
(11) Kozlowski, J. T.; Davis, R. J. Sodium modification of zirconia catalysts for ethanol coupling to 1-butanol. *J. Energy Chem.* **2013**, *22*, 58−64.
(12) Auepattana-aumrung, C.; Wannapaiboon, S.; Wannakao, S.; Praserthdam, S.; Jongsomjit, B.; Panpranot, J.; Praserthdam, P. A study of the acidity on catalyst surface to control 1-butene reaction mechanism of metallosilicate catalysts. *Mol. Catal.* **2022**, *529*, No. 112533.
(13) Yang, C.; Meng, Z. Y. Bimolecular Condensation of Ethanol to 1-Butanol Catalyzed by Alkali Cation Zeolites. *J. Catal.* **1993**, *142*, 37−44.
(14) Scalbert, J.; Thibault-Starzyk, F.; Jacquot, R.; Morvan, D.; Meunier, F. Ethanol condensation to butanol at high temperatures over a basic heterogeneous catalyst: How relevant is acetaldehyde self-aldolization? *J. Catal.* **2014**, *311*, 28−32.
(15) Ho, C. R.; Shylesh, S.; Bell, A. T. Mechanism and Kinetics of Ethanol Coupling to Butanol over Hydroxyapatite. *ACS Catal.* **2016**, *6*, 939−948.
(16) Zuo, Y.; Li, Y.; Li, J.; Zhang, X.; Liao, H.; Wang, Y.; Yang, W. Novel bio-composite of hydroxyapatite reinforced polyamide and polyethylene: Composition and properties. *Mater. Sci. Eng., A* **2007**, *452-453*, 512−517.
(17) Wu, X.; Fang, G.; Liang, Z.; Leng, W.; Xu, K.; Jiang, D.; Ni, J.; Li, X. Catalytic upgrading of ethanol to n-butanol over M-CeO_2/AC (M = Cu, Fe, Co, Ni and Pd) catalysts. *Catal. Commun.* **2017**, *100*, 15−18.
(18) Jiang, D.; Wu, X.; Mao, J.; Ni, J.; Li, X. Continuous catalytic upgrading of ethanol to n-butanol over Cu-CeO_2/AC catalysts. *Chem. Commun.* **2016**, *52*, 13749−13752.
(19) Pinthong, P.; Praserthdam, P.; Jongsomjit, B. Effect of Calcination Temperature on Mg-Al Layered Double Hydroxides (LDH) as Promising Catalysts in Oxidative Dehydrogenation of Ethanol to Acetaldehyde. *J. Oleo Sci.* **2019**, *68*, 95−102.
(20) Marcu, I.-C.; Tanchoux, N.; Fajula, F.; Tichit, D. Catalytic Conversion of Ethanol into Butanol over M−Mg−Al Mixed Oxide Catalysts (M = Pd, Ag, Mn, Fe, Cu, Sm, Yb) Obtained from LDH Precursors. *Catal. Lett.* **2012**, *143*, 23−30.
(21) Perrone, O. M.; Lobefaro, F.; Aresta, M.; Nocito, F.; Boscolo, M.; Dibenedetto, A. Butanol synthesis from ethanol over CuMgAl mixed oxides modified with palladium (II) and indium (III). *Fuel Process. Technol.* **2018**, *177*, 353−357.
(22) Ogo, S.; Onda, A.; Yanagisawa, K. Selective synthesis of 1-butanol from ethanol over strontium phosphate hydroxyapatite catalysts. *Appl. Catal., A* **2011**, *402*, 188−195.
(23) Ogo, S.; Onda, A.; Iwasa, Y.; Hara, K.; Fukuoka, A.; Yanagisawa, K. 1-Butanol synthesis from ethanol over strontium phosphate hydroxyapatite catalysts with various Sr/P ratios. *J. Catal.* **2012**, *296*, 24−30.
(24) Huang, J.; Chen, C.; Huang, Z.; Yao, D.; Wu, C.; Cheng, Y. Self-assembly pore-forming mechanism of foam boundary templates and the preparation of porous strontium hydroxyapatite microspheres by homogeneous precipitation. *CrystEngComm* **2019**, *21*, 5658−5664.
(25) Sun, Z.; Couto Vasconcelos, A.; Bottari, G.; Stuart, M. C. A.; Bonura, G.; Cannilla, C.; Frusteri, F.; Barta, K. Efficient Catalytic Conversion of Ethanol to 1-Butanol via the Guerbet Reaction over Copper- and Nickel-Doped Porous. *ACS Sustainable Chem. Eng.* **2016**, *5*, 1738−1746.
(26) Tangy, A.; Pulidindi, I. N.; Dutta, A.; Borenstein, A. Strontium Oxide Nanoparticles for Biodiesel Production: Fundamental Insights and Recent Progress. *Energy Fuels* **2021**, *35*, 187−200.
(27) Shahraini, N.; Entezari, M. H. Biodiesel from waste oil under mild conditions by a combination of calcium-strontium oxide nanocatalyst and ultrasonic waves. *Int. J. Energy Res.* **2022**, *46*, 13781−13800.
(28) Cimino, S.; Lisi, L.; Romanucci, S. Catalysts for conversion of ethanol to butanol: Effect of acid-base and redox properties. *Catal. Today* **2018**, *304*, 58−63.
(29) Al-Saadi, A.; Mathan, B.; He, Y. Biodiesel production via simultaneous transesterification and esterification reactions over SrO−ZnO/Al_2O_3 as a bifunctional catalyst using high acidic waste cooking oil. *Chem. Eng. Res. Des.* **2020**, *162*, 238−248.
(30) Seekhiaw, P.; Pinthong, P.; Praserthdam, P.; Jongsomjit, B. Optimal Conditions for Butanol Production from Ethanol over MgAlO Catalyst Derived from Mg-Al Layer Double Hydroxides. *J. Oleo Sci.* **2022**, *71*, 141−149.
(31) Yuan, B.; Zhang, J.; An, Z.; Zhu, Y.; Shu, X.; Song, H.; Xiang, X.; Wang, W.; Jing, Y.; Zheng, L.; He, J. Atomic Ru catalysis for ethanol coupling to C4+ alcohols. *Appl. Catal., B* **2022**, *309*, No. 121271.
(32) Elhalil, A.; Qourzal, S.; Mahjoubi, F. Z.; Elmoubarki, R.; Farnane, M.; Tounsadi, H.; Sadiq, M.; Abdennouri, M.; Barka, N. Defluoridation of groundwater by calcined Mg/Al layered double hydroxide. *Emerging Contam.* **2016**, *2*, 42−48.
(33) Valihura, K. V.; Larina, O. V.; Kyriienko, P. I.; Yaremov, P. S.; Khalakhan, I.; Trachevskiy, V. V.; Soloviev, S. O.; Orlyk, S. M. Fast synthesis of MgO−Al2O3 systems: effect on physicochemical characteristics and catalytic properties in Guerbet condensation of ethanol. *Appl. Nanosci.* **2023**, 1−14.
(34) Larina, O. V.; Kyriienko, P. I.; Shcherban, N. D.; Yaremov, P. S.; Balakin, D. Y.; Khalakhan, I.; Veltruská, K.; Soloviev, S. O.; Orlyk, S. M. Carbon-Supported Mg−Al Oxide Hybrid Catalysts for Aqueous Ethanol Conversion into 1-Butanol in a Flow Reactor. *Ind. Eng. Chem. Res.* **2021**, *60*, 11964−11976.
(35) Zhang, J.; Shi, K.; An, Z.; Zhu, Y.; Shu, X.; Song, H.; Xiang, X.; He, J. Acid−Base Promoted Dehydrogenation Coupling of Ethanol on Supported Ag Particles. *Ind. Eng. Chem. Res.* **2020**, *59*, 3342−3350.
(36) Zhao, H.; Shen, X.; He, J.; Kou, J.; Tao, T.; Can, Y.; Huang, H.; Jiang, D.; Lin, L.; Li, X. Catalytic upgrading of ethanol to higher

https://doi.org/10.1021/acsomega.3c03752
ACS Omega 2023, 8, 32775−32783

alcohols over ordered mesoporous Cu-La-Al composite metal oxides. *Appl. Surf. Sci.* **2022**, *599*, No. 153851.
(37) Pinzón, M.; Cortés-Reyes, M.; Herrera, C.; Larrubia, M. Á.; Alemany, L. J. Ca-based bifunctional acid-basic model-catalysts for n-butanol production from ethanol condensation. *Biofuels, Bioprod. Biorefin.* **2020**, *15*, 218−230.
(38) Mehta, K.; Jha, M. K.; Divya, N. Statistical optimization of biodiesel production from Prunus armeniaca oil over strontium functionalized calcium oxide. *Res. Chem. Intermed.* **2018**, *44*, 7691−7709.
(39) Sarmin, S.; Ethiraj, B.; Tarek, M.; Rengaraju, B.; Karim, K. M. R.; Ong, H. R.; Abdullah, H.; Khan, M. M. R. Palm Oil Derived Alkyd Resin Synthesis Catalyzed by $SrOSr(OH)_2$ Nanoparticles. *J. Crit. Rev.* **2020**, *7*, 2131−2139.
(40) Li, H.; Liu, F.; Ma, X.; Wu, Z.; Li, Y.; Zhang, L.; Zhou, S.; Helian, Y. Catalytic performance of strontium oxide supported by MIL−100(Fe) derivate as transesterification catalyst for biodiesel production. *Energy Convers. Manage.* **2019**, *180*, 401−410.
(41) Kang, M.-J.; Choi, S.-Y. Preparation of Sr_2CeO_4 blue phosphor by ultrasonic spray pyrolysis: effect of NH_4NO_3 addition. *J. Mater. Sci.* **2002**, *37*, 2721−2729.
(42) SING, K. S. W. Reporting Physisorption Data for Gas/Solid Systems. *Pure Appl. Chem.* **1982**, *54*, 2201−2218.
(43) Thommes, M.; Kaneko, K.; Neimark, A. V.; Olivier, J. P.; Rodriguez-Reinoso, F.; Rouquerol, J.; Sing, K. S. W. Physisorption of gases, with special reference to the evaluation of surface area and pore size distribution (IUPAC Technical Report). *Pure Appl. Chem.* **2015**, *87*, 1051−1069.
(44) Chen, K.; Zhang, T.; Chen, X.; He, Y.; Liang, X. Model construction of micro-pores in shale: A case study of Silurian Longmaxi Formation shale in Dianqianbei area, SW China. *Pet. Explor. Dev.* **2018**, *45*, 412−421.
(45) Cychosz, K. A.; Thommes, M. Progress in the Physisorption Characterization of Nanoporous Gas Storage Materials. *Engineering* **2018**, *4*, 559−566.
(46) Sotomayor, F. J.; Cychosz, K. A.; Thommes, M. Characterization of Micro/Mesoporous Materials by Physisorption: Concepts and Case Studies. *Acc. Mater. Surf. Res.h* **2018**, *3*, 34−50.
(47) Di Cosimo, J. I.; Apesteguıa, C. R.; Ginés, M. J. L.; Iglesia, E. Structural Requirements and Reaction Pathways in Condensation Reactions of Alcohols on Mg_yAlO_x Catalysts. *J. Catal.* **2000**, *190*, 261−275.
(48) Xiao, Y.; Li, X.; Yuan, Z.; Li, J.; Chen, Y. Catalytic Dehydration of Ethanol to Ethylene on TiO_2/4A Zeolite Composite Catalysts. *Catal. Lett.* **2009**, *130*, 308−311.
(49) Tresatayawed, A.; Glinrun, P.; Jongsomjit, B. Ethanol Dehydration over WO_3/TiO_2 Catalysts Using Titania Derived from Sol-Gel and Solvothermal Methods. *Int. J. Chem. Eng.* **2019**, *2019*, 1−11.
(50) Weishen Yanga, Y. K.; Kim, Y.; Lui, P. K. T.; Sahimia, M.; Tsotsisa, T. T. A study by in situ techniques of the thermal evolution of the structure of a Mg-Al-CO_3- layered double hydroxide. *Chem. Eng. Sci.* **2002**, *57*, 2945−2953.
(51) Campisano, I. S. P.; Rodella, C. B.; Sousa, Z. S. B.; Henriques, C. A.; Teixeira da Silva, V. Influence of thermal treatment conditions on the characteristics of Cu-based metal oxides derived from hydrotalcite-like compounds and their performance in bio-ethanol dehydrogenation to acetaldehyde. *Catal. Today* **2018**, *306*, 111−120.
(52) Ahmed, R.; Sinnathamb, C. M.; Subbarao, D. Kinetics of Decoking of Spent Reforming Catalyst. *J. Appl. Sci.* **2011**, *11*, 1225−1230.

https://doi.org/10.1021/acsomega.3c03752
ACS Omega 2023, 8, 32775−32783